WTC 2018 - Dubai

wtc2018.ae

Paper Submission Sample

Numerical analyses for the design of fiber reinforced precast concrete lining segments for ram thrust forces

Paolo Cucino [1], Dimitri Rizzardi [2], Luca Schiavinato [3] and Alberto Meda [4]

1 SWS Engineering S.p.A., p.cucino@swsglobal.com

2 SWS Engineering S.p.A., d.rizzardi@swsglobal.com

3 SWS Engineering S.p.A., l.schiavinato@swsglobal.com

4 University of Rome Tor Vergata, alberto.meda@uniroma2.it

ABSTRACT

Fibre reinforcement is increasingly used in civil works to improve materials strength against brittle failure mode. In mechanized tunnelling, precast concrete lining design and reinforcement dimensioning is carried out according to various loading schemes covering to the entire service life of segments and rings. One of the most onerous load conditions is related to the longitudinal ram forces need to the TBM advancement, which determines a considerable amount of localized reinforcement.

This paper describes the design of two sets of precast concrete lining of approximately 10m diameter which differ for segment geometry and number of rams. The paper highlights how the use of steel-fibre reinforcement against the ram thrust forces load can provide several advantages and economies, not just regarding TBM advance stage but also for production and logistic, i.e. easier production and assembly of the conventional reinforcement cage due to simpler geometry, and higher performance during handling and positioning.

Key Words: Fibre reinforced concrete, Constitutive model, Numerical simulation, Non-linear analysis.

1. INTRODUCTION

The mechanized excavation of tunnels is gradually evolving toward more versatile solutions. An example is the possibility of boring large tunnels in different geological conditions (e.g. from soft soil to hard rock) with a single machine.

A precast segmental concrete liner is usually installed at the back of the shielded machines (Tunnel Boring Machines or shields). The circular shape guarantees a better static behaviour than the horse shaped-sections adopted in conventional excavations. The ring is compressed and bending stresses are usually very limited. The installation consists in the sequential assembly of its constituent segments. To avoid the system instability, segments are connected to each other as well to the previous ring ones. Once the ring is closed, a backfill is grouted to ensure the confinement and to regularize the load application from the ground to the liner.

The design of the supporting system can be based on empirical or analytical formulations. Every loading condition experienced by the segment must be considered: from formwork removal phase to the operating phase in the long term.

Focusing on the Tunnel Boring Machines, there are two commercial possibilities. The first is to use a TBM realized ex novo. The second is to use a reconditioned machine sets according to the current requirements. Formworks and parts of the prefabrication plant are usually re-utilized together with a reconditioned TBM. This second case is the one examined in this paper, i.e. the typology of the TBM is pre-defined and minor changes can be implemented:

- the typology of the segment is defined according to the type of the available machine and formworks;

- it is possible to detail the design procedure of the precast segments.

In this context, it has been tested the use of steel-fibre reinforced elements. Fibre reinforced materials are experiencing a fast pulse and development thanks to the new scientific and technological achievements that allow:

- to develop approaches for the definition of their material properties;
- to verify the behaviour at large scale through physical models;
- to define the computation and test methodologies following the most recent national and international guidelines;
- to validate numerical modelling through non-linear analyses.

The paper presents the procedure and numerical analyses carried out for the dimensioning of fibre reinforced precast concrete lining segments for ram thrust forces. These forces generally have high values, because they must overcome the rock resistance at face and the TBM weight and the soil friction at the contour of the shield. In the following it is highlighted the need of representing the real geometry of the segment and the load foot print application, in order to obtain sufficiently reliable values of radial and circumferential traction stresses.

It is important to point out the influence of circumferential stresses generated by thrust jacks. Some designers consider them negligible because of the confinement given by the adjacent segments of the ring. This paper shows (in accordance with several international guidelines) the relevance of these stresses in the definition of the stress field of each precast segment. In the design phase, the information obtained by these analyses should contribute to the definition of the features of the boring machine and of the resistant model capable of absorbing those stresses.

2. FIBER REINFORCED CONCRETE PROPERTIES

The fibre reinforced concrete (FRC) adopted is classified according to the Model Code 2010. Considering the similarities of the compression behaviour of the FRC and of the concrete matrix without fibres, the reference for the compressive properties is the Italian regulation D.M.2008.

In order to classify the FRC according to Model Code 2010, it is necessary to refer to two parameters: f_{R1k} and f_{R3k}. The constitutive law for the material at CASE I showed in Fig. (1), the value of the resistance f_{ct} till the peak point is the same as the concrete in simple tension condition, defined as the Eqs. (1) to (2) below:

$$\sigma_{ct} = E_{ci} \cdot \varepsilon_{ct} \qquad \text{for } \sigma_{ct} \le 0.9 \cdot f_{ctm} \tag{1}$$

$$\sigma_{ct} = f_{ctm} \cdot \left(1 - 0.1 \frac{0.00015 - \varepsilon_{ct}}{0.00015 - 0.9 \cdot f_{ctm} / E_{ci}} \right) \qquad \text{for } 0.9 \cdot f_{ctm} \le \sigma_{ct} \le f_{ctm} \tag{2}$$

with the modulus E_{ci} calculated according the Eq. (3):

$$E_{ci} = E_{c0} \cdot \alpha_E \cdot \left(\frac{f_{ck} + \Delta f}{10} \right)^{1/3} \tag{3}$$

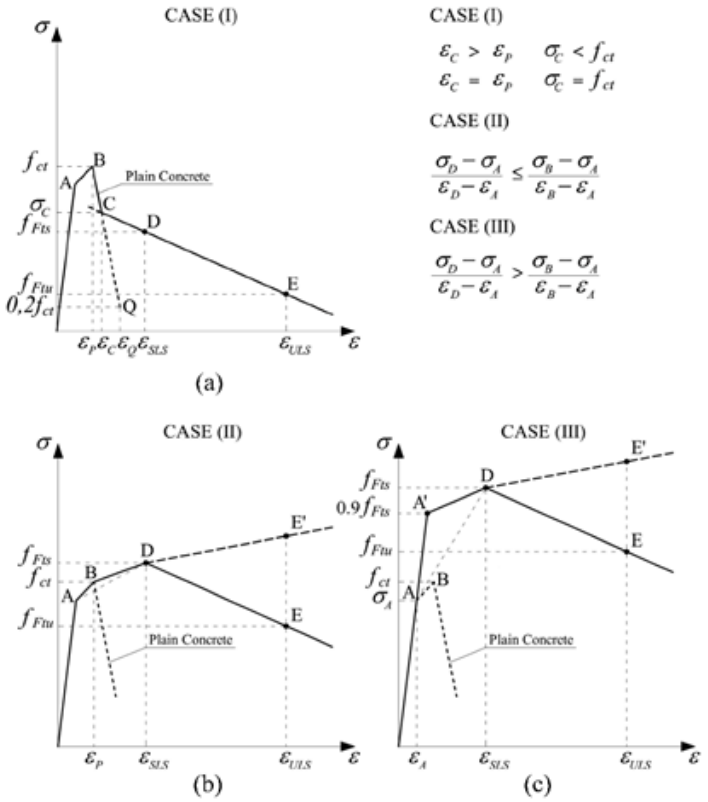

Figure 1. Stress-strain relations at SLS for softening behavior of FRC according to the Model Code 2010

The points A and B are defined as:

$$\varepsilon_A = 0.9 \cdot \frac{f_{ct}}{E_{ci}} \qquad \sigma_A = 0.9 f_{ct} \tag{4}$$

$$\varepsilon_B = \varepsilon_P = \qquad \sigma_B = \sigma_{ct}(\varepsilon_B) a \tag{5}$$

The post peak tree is described through the following function

$$\frac{\sigma - f_{ct}}{0.2 f_{ct} - f_{ct}} = \frac{\varepsilon - \varepsilon_P}{\varepsilon_Q - \varepsilon_P} \qquad \text{for} \qquad \varepsilon_P \le \varepsilon \le \varepsilon_C \tag{6}$$

where

$$\varepsilon_Q = \frac{G_F}{f_{ct} \cdot l_c} + \left(\varepsilon_P - \frac{0.8 f_{ct}}{E_{ci}} \right) \tag{7}$$

The forth segment of the tension-deformation diagram is described by two points with coordinates (ε_{SLS} , f_{Fts}) and (ε_{ULS} , f_{Ftu}). For numerical modelling, these values are defined as a function of the characteristic dimension of the mesh l_c:

$$\varepsilon_{SLS} = CMOD_1 / l_c \tag{8}$$

$$\varepsilon_{ULS} = w_u / l_c \tag{9}$$

For the examined problems, the concrete resistance class for compression is C50/60, and the FRC class adopted is 4.0 C, with characteristic resistance f_{R1k} higher than 4.0 MPa and ratio between

the range $0.9 \leq f_{R3k} / f_{R1k} \leq 1.1$. Consequently, the characteristic strength f_{R3k} will be higher than f_{R3k} =0.9* f_{R1k} =3.6 MPa. The fibre typology applied is DRAMIX 4D 80/60 BG. Tests conducted by the producer show that this product has a resistance f_{R1k} = 4.0 MPa, thanks to the high tensile resistance, ductility and anchoring capacity values of steel fibres. The ductility and the anchoring capacity are targeted to be effective on $0.1 \div 0.3$ mm cracks. The result is a durable and watertight structure. The 4D series is also the ideal solution for combining steel fibres and other reinforcement methods. The properties of the steel fibres are reported in the Tab.(1).

The connected properties of fibre reinforced concrete are illustrated in the Tab.(2).

Table 1. Features of DRAMIX 4D 80/60 BG fibres

Parameter	Reference values
Length	60 mm
Diameter	0.75 mm
Aspect ratio (l/d)	80
Minimum tensile strength	> 1800 MPa
Ultimate elongation	< 4%

Table 2. Parameters of the FRC adopted

Parameter	Reference values
Compressive strength class	C50/60
Characteristic compressive cylinder strength of concrete at 28 days	f_{ck} = 50 MPa
Partial factor for concrete	γ_C = 1.5
Design value of concrete compressive strength (long term)	f_{cd} = 33.33 MPa
Design value of concrete compressive strength (short term)	f_{cd} = 28.33 MPa
Characteristic residual strength of FRC for CMOD = 0.5 mm	f_{R1k} = 4.0 MPa
Characteristic residual strength of FRC for CMOD = 2.5 mm	f_{R3k} = 3.6 MPa
Tensile ultimate residual strength for the rigid-plastic model	f_{Ftuk} = 1.2 MPa
Partial safety factor for the tensile strength of FRC	γ_F = 1.5

Finally, the constitutive law used in the numerical models was defined according to a mesh reference dimension equal to 4.0cm, and the calculated values are reported in Tab.(3). Looking at the compressive strength, the material is considered linear elastic until the resistance limit equal to f_{cd} at 0.35%. The stress-strain relation, at the Ultimate Limit State, for the fibre-reinforced material is defined according to paragraph 5.6.5 of the Model Code 2010.

Table 3. Tensile stress-strain relation for fibre reinforced segments. Reference points

ε [-]	σ_t [MPa]
0.000000	0.000
0.000067	2.570
0.000150	2.850
0.000507	2.210
0.002000	1.544

The constitutive law for the steel reinforcements is assumed as linear perfectly plastic.

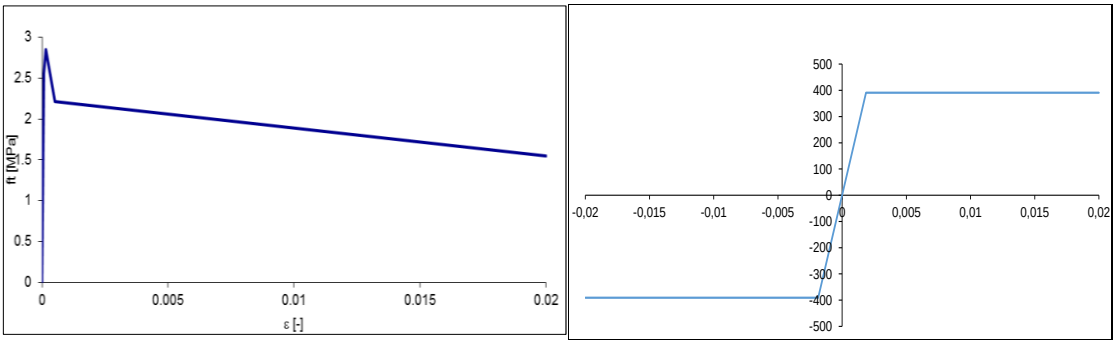

Figure 2. Tensile stress-strain relation for fiber reinforced segments and steel reinforcements

3. BASIC PROPERTIES OF CONSTITUTIVE MODEL AND NUMERICAL VALIDATIONS

In order to demonstrate the reliability of the simulation, highlighting the correct behaviour of the model in terms of adherence to the constitutive link implemented, two virtual samples characterized by different strain states have been analysed:

- the first is made up of a 100x100 mm cross-sectional concrete bar, in which a half-carving is made to reduce the 90x90 mm section (in order to generate a localized weakening). The contour conditions provide a fixity on the right side and a displacement imposed at the left end of the bar. The stress condition in the component being analysed is therefore of uniform traction;
- the second sample has the purpose of examining the behaviour in a multi-axial stress condition. The simulation was carried out using the same concrete segment base model (after removing the reinforcement) which will be described in detail in the following chapters. In this case the focus was focused on the area between the two loading plates, where the tensions of spalling assume a regular pattern almost tangential.

The numerical models have been carried out by the ABAQUS code models. the concrete volume is discretized into 8 node solid elements (C3D8R). The ”concrete damage plasticity” model of ABAQUS is used to describe the nonlinear material behaviour of concrete, according to the use of the concrete damage plasticity model associated to the non-linear resistance law according to the Tab.(3).

This solution, which is widely used in the modelling of structural elements in concrete and reinforced concrete, is particularly efficient from a numerical point of view and is characterized by a failure domain defined in the space of effective tensions through a surface obtained by combining the well-known Drucker-Prager and Rankine (isotropic damage and a non-associated plastic flow)

In addition to the reference diagram σ-ε, this behaviour model requires the definition of the following parameters

- dilatancy angle: $\Psi = 30°$ (Lee & Fenves, 1998)
- resistance ratio: $\alpha_f = f_{b0} / f_{c0} = 1.16$ (Kupfer & Gerstle, 1973)
- parameter of the flow potential G: $\varepsilon = 0.10$
- second stress invariant ratio: $K_c = 2/3 = 0.667$

The compression and tension damage variables (d_c and d_t drift) were not assigned, given that the simulation carried out reproduces a monotone load process (therefore, it may exclude cyclic damage phenomena).

Considering the implemented simulation, the problem solution was handled using the nonlinear solver designed for static or quasi-static structural analyses. In this way, it was possible to take into account the non-linearity of the constituent ties made for the materials and contacts used to define the outline conditions.

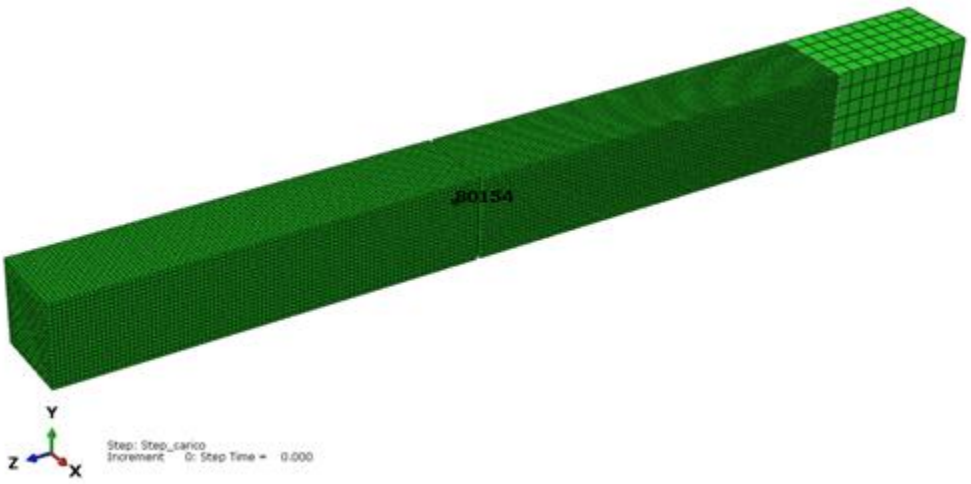

Figure 3. Validation model no.1

The interpretation of the analysis carried out following the stress path of one of the finite elements located within the area affected by the crackling phenomenon, produced results matching the provided behaviour.

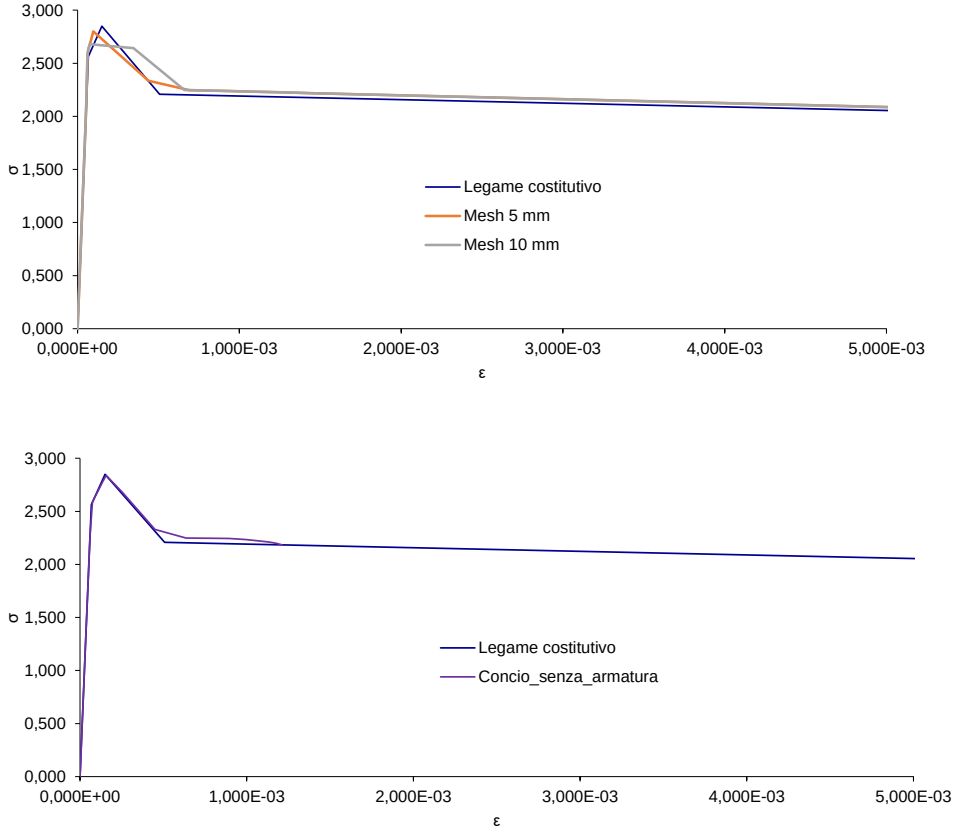

Figure 4. Results of numerical model behavior. Comparison between the measured value and the theoretical data for the first model (above) and the second model (below)

4. CASES STUDIES

4.1. TBM and Lining ring typology

4.1.1. Case 1

The tunnel is bored with a shielded Dual Mode TBM. This machine is studied to cope with both hard rocks and non-cohesive material (sand and breccia), allowing the excavation in the very variable geotechnical and geomechanical conditions along the track. The characteristics of the installed liner ring are below reported:

- internal diameter 9.60m
- element thickness 0.35m
- ring typology 8+0 elements (big key)
- number of thrust groups 24 groups of two jacks each (three groups per segment).

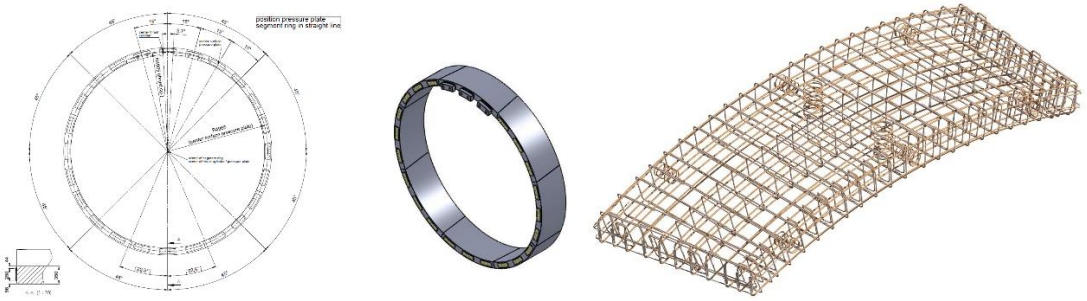

Figure 5. Scheme of the precast segments liner of Case 1 and associated standard segment reinforcement

4.1.2. Case 2

The tunnel is bored with a shielded EPB TBM. This machine is designed to cope with both sound rock and non-cohesive material below the water table, allowing the excavation in variable geotechnical conditions along the track. The characteristics of the installed liner ring are:

- internal diameter 9.60m
- element thickness 0.32m
- ring typology 6+1 elements
- number of thrust groups 13 groups of three jacks each (two groups per segment).

Figure 6. Scheme of the precast segments liner of Case 2 and associated standard segment reinforcement

4.2. Numerical models

A solid nonlinear model, realized and computed using the ABAQUS code, is considered for the analyses. The 3D geometry of the segment is generated with the extrusion of the transversal section. The surface is subdivided and sectioned in order to identify the zones loaded by the jacks and to differentiate the boundary conditions. The decomposition of the geometry into sub regions is a preliminary condition to obtain a regular and consistent mesh of the model, an essential requirement for achieving reliable results. The importance of the density and regularity of the mesh has already been pointed out. For the segment, finite solid C3D8R elements (8-node linear brick, reduced integration, hourglass control) with maximum dimension of 40x40x40 mm3 are adopted. For the lateral supports a denser mesh of the same C3D8R elements is adopted, to achieve a higher precision in these contact zones. The maximum dimension of the elements is 25x25x25 mm^3.

To simulate the interaction given by the adjacent segments, the segment extremities are supported by a hard contact interaction at the interface with lateral segments and springs for the contact with the previous installed rings. Where provided, the reinforcements has been simulated as embedded elements which allow the perfect adherence between the concrete and the reinforcement.

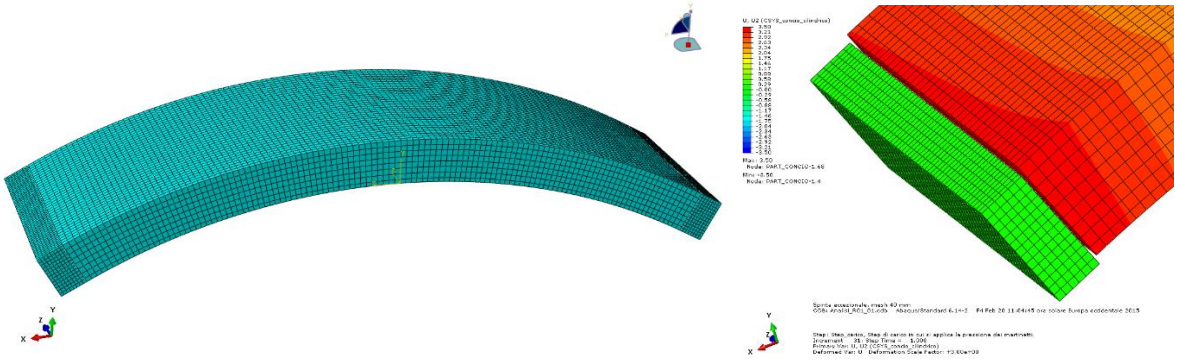

Figure 7. Results of numerical model behavior. Detail showing the detachment allowed by the contact elements

The design condition defines a maximum thrust force (exceptional condition n) of N_{tot}= 100 MN on the whole ring for both the analysed cases. The load is applied in different way: three groups per segment for the case 1 and two groups per segment for the case 2.

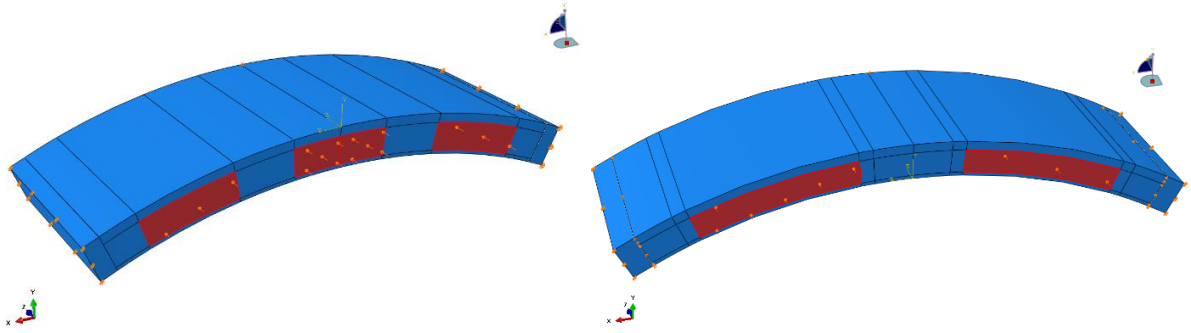

Figure 8. Applied force. Thrust group for the case 1 (left) and case 2 (right)

4.3. Load application and obtained results

4.3.1. Case 1

The analysis for the theoretical conditions (N= N_{tot}, no reinforcement) showed convergence, and in relation to the tension and displacement obtained the structural element is suitable for its function. For a better understanding of the functioning of the system, the loading has been incremented up to the instability condition. The results of the computation converge until a maximum ram force of 122,500 kN (+22.5%) on the entire ring.

Considering the theoretical load condition, the maximum circumferential traction is showed in the portion between the contact plates. These tensile zones are rather superficial. Below the plates, stresses do not exceed the tensile peak resistance of the material, which remain in the elastic field. Similar stress values are reached in the lateral zones.

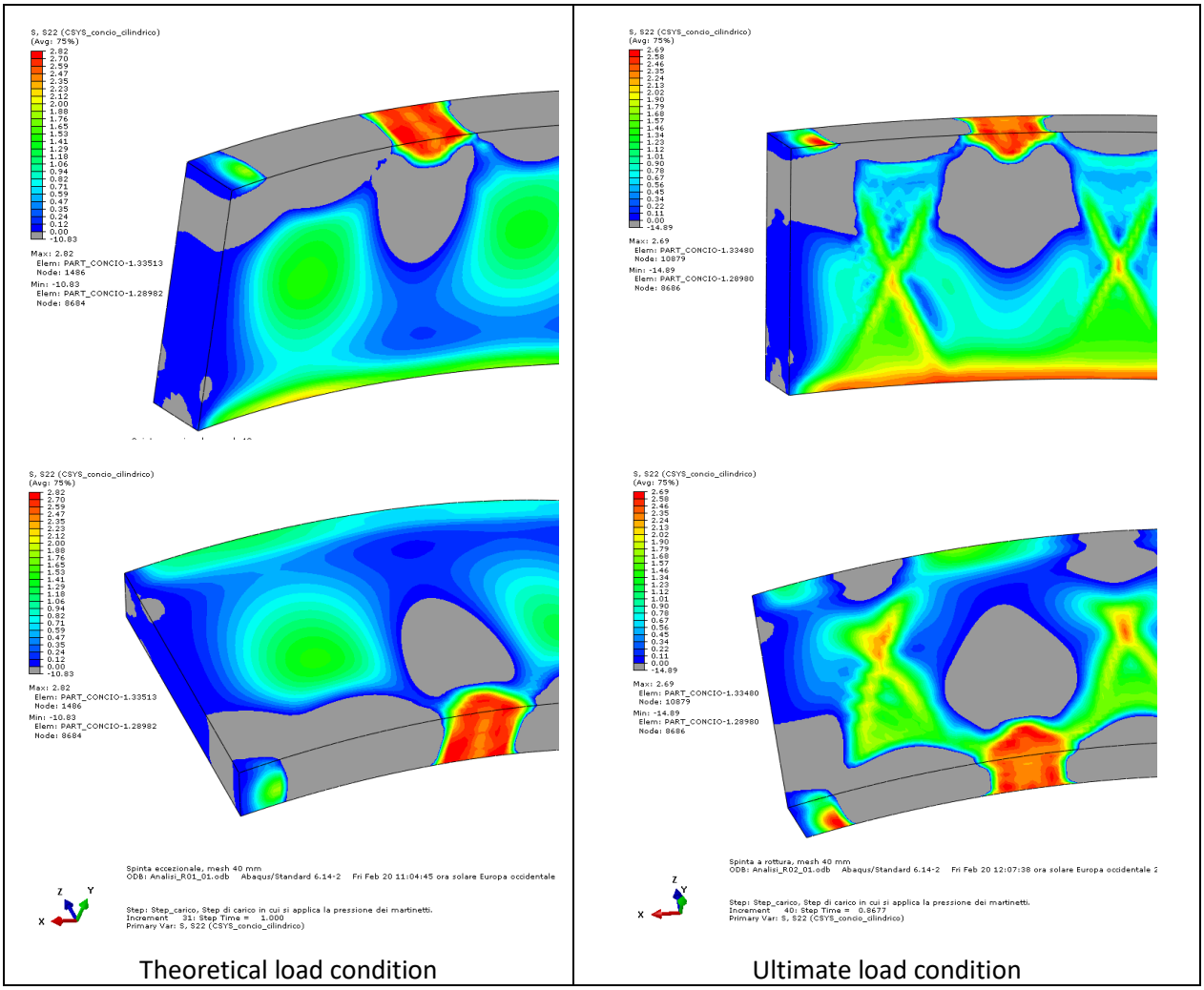

Figure 9. Comparison between circumferential traction in standard and ultimate conditions, Case 1

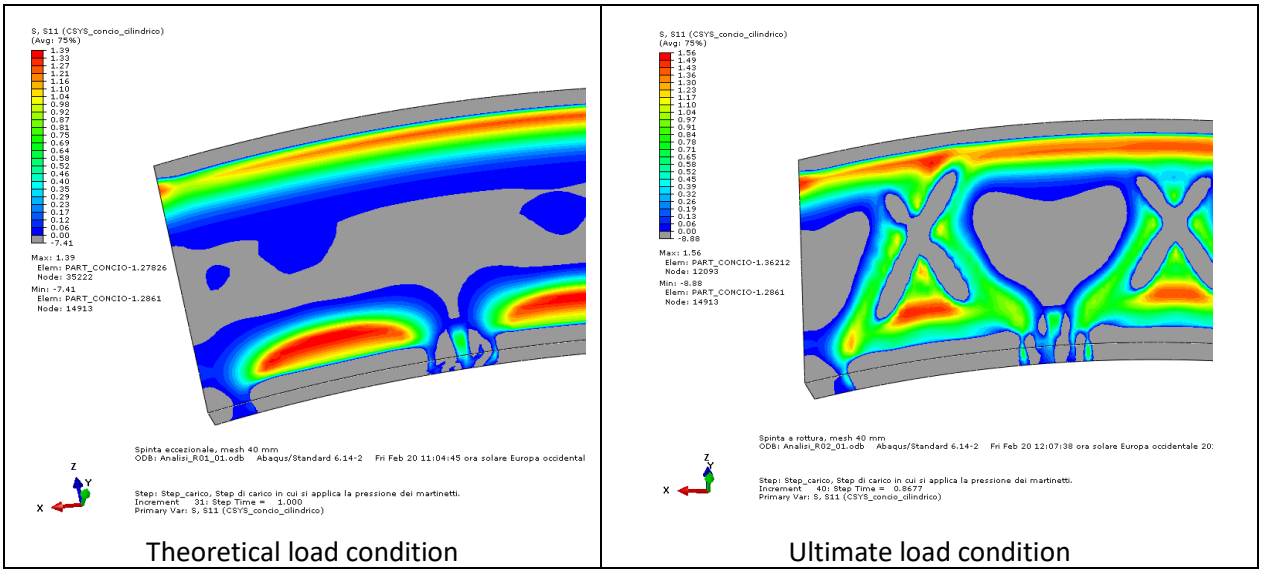

Figure 10. Comparison between radial traction in standard and ultimate conditions, Case 1

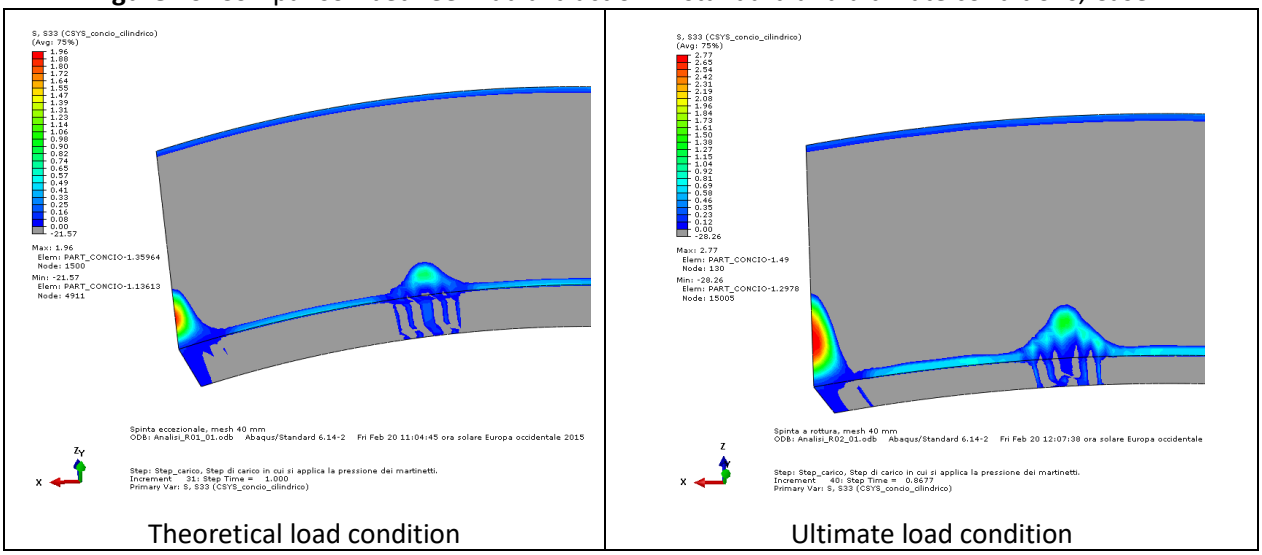

Figure 10. Comparison between longitudinal traction in standard and ultimate conditions, Case 1

4.3.2. Case 2

The acting load is given by the total thrust force spread for the number of segments and the two loading group. Opposite than the case 1, the computation does not reach the convergence. The stability is achieved for a loading equal to the 85% of the design value.

In order to reach the design load value, two possible solutions are analysed:

- increase the size of the loading plates;
- adoption of a mixed reinforcement system.

The first solution implies an enlargement of about 50cm (25cm per side) of the loading zones, consequently the tensile zones are reduced. The cost of this solution is a limitation of the operability of the machine. The second solution has been considered the more effective, also considering the slenderness of the segment. The results obtained for the mixed reinforcement system are presented in the next subsection

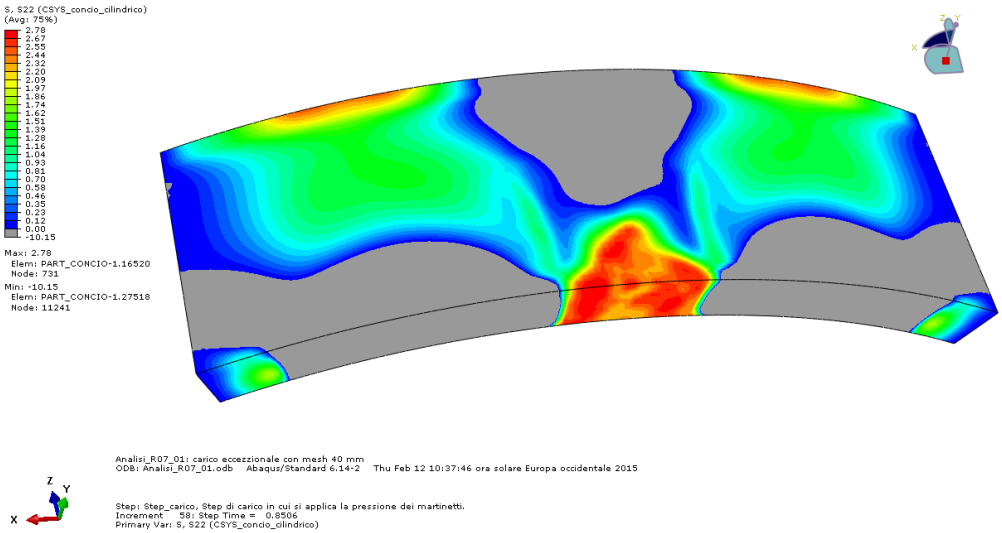

Figure 11. Circumferential traction in the ultimate condition at the 85% of N_{tot}, Case 2

The reinforcement in question, are modelled using axial load resisting elements (truss) "embedded" in the solid element mesh. The nodes of the monodimensional elements are merged with the nodes of the tridimensional ones, ensuring the congruence of the displacements and strains. The analysis show a significant improvement in the behaviour of the segment, which can now support the application of the entire design load

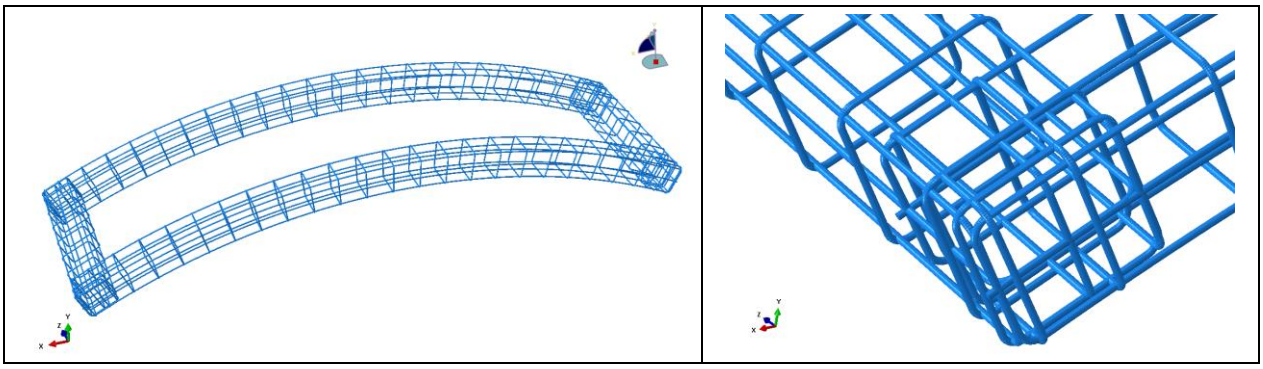

Figure 12. Geometry of the monodimensional element composing the reinforcement

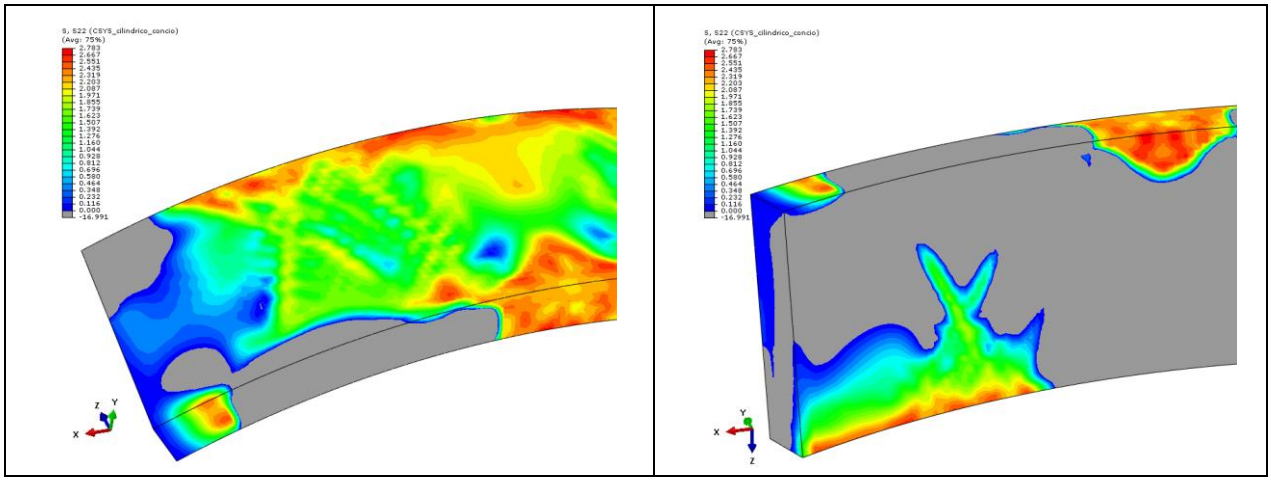

Figure 13. Circumferential traction at the intrados and extrados in standard condition, Case 2

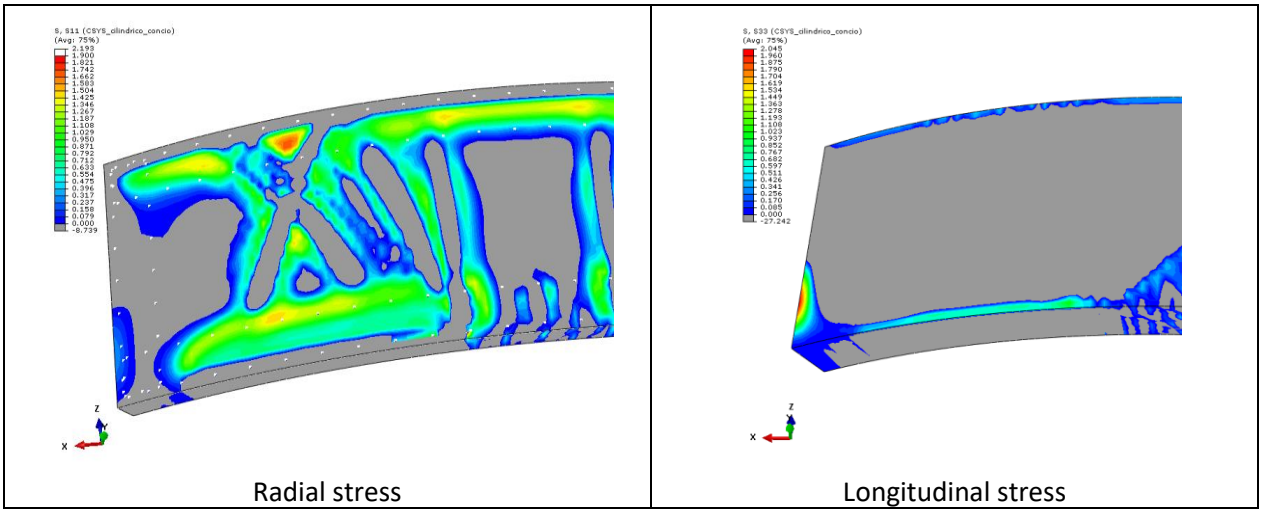

Figure 11. Radial and longitudinal traction in standard condition, Case 2

5. CONCLUSION

This paper has illustrated the procedure carried out in order to check the behaviour of precasted concrete segments under the action of ram load during the TBM advance. Through modern technologies it is possible to carry out realistic simulations of the behaviour under the action of such thrusts in a realistic manner. At the same time, material research is gradually allowing the use of fibre-reinforced materials instead of conventional reinforcements, in order to simplifying the prefabrication procedures acting a complete, or partial, substitution of the traditional reinforcement with diffused steel fibres. For these materials, the procedure for defining the reference parameters for the definition of tensile behaviour has been described, associated to the verification carried out and the comparison to the theoretical curve.

Two cases, with a similar geometry and thrust systems, were analysed. Their comparison is based on the circumferential stresses, which are the most critical and influence the structural dimensioning. In the first case the segment is pushed by 3 thrust groups. Results show a gradual increase of the stresses and of the material exploitation. In this condition it is possible to completely replace the traditional reinforcement with the diffused one. In the second case only 2 thrust groups for each segment are provided. With a load level similar to that of case 1, the numerical simulation generates unstable results, due to failure occurring in the central zone of the segment. With the addition of perimetral reinforcement, the fibre-reinforced material is effectively exploited, in similarity to case 1, and the segment is verified. Even if such perimetral reinforcement is not taken into account in the structural bending checks, it is important to consider it for the local analysis of contact zones.

The numerical modelling highlights the possibility of optimizing the design solution, or the need for special intervention due to the real load conditions resulting from a different distribution of loading foot.